XI International Conference on Computational Plasticity. Fundamentals and Applications
COMPLAS XI
E. Oñate, D.R.J. Owen, D. Peric and B. Suárez (Eds)

EXPERIMENTALLY-BASED IDENTIFICATION OF SHEET METALS PLASTIC ANISOTROPY, WITH A VIEW TO OBTAINING IMPROVED PREDICTIONS IN FORMING SIMULATIONS

G. FERRON, I. CHARPENTIER, M. MARTINY, M. TEACA

Laboratoire d'Étude des Microstructures et de Mécanique des Matériaux, LEM3, UMR CNRS 7239,
Université Paul Verlaine - Metz, Ile du Saulcy, 57045 Metz, France

E-mail: gerard.ferron@univ-metz.fr

Key words: Sheet Metals, Plastic Anisotropy, Experimental Characterization.

Summary. Experimental tests developed to characterize sheet metals plastic anisotropy are reviewed in this paper, with particular emphasis on those dedicated to the identification of advanced yield surfaces capable of improving the predictions in forming simulations. The direct identification methods using a variety of tests that cover a wide range of proportional stress states are first discussed. Inverse methods based on experiments on complex-shaped specimens are next presented. With these methods, the parameters of a selected material model are determined by minimizing the discrepancies between numerically-predicted results and experimental ones.

1 INTRODUCTION

Sheet metal forming processes are widely used in automotive and domestic appliance industries to manufacture complex-shaped structural components. In view of the complexity of textural and micro-structural evolutions associated with plastic yielding, the optimization of these processes should be performed by means of finite element (FE) simulations in which only the most important aspects of anisotropic plasticity are selected in relation with the expected predictions.

In addition to the initial yield surface, two main kinds of surfaces can be defined in stress space, depending on the experimental procedure applied for their determination.

The subsequent yield surfaces (SYSs) are obtained by exploring the whole stress space after a given pre-strain has been applied to the material. The determination of SYSs reveals the anisotropic character of strain-hardening. The Bauschinger effect is one of the manifestations of anisotropic hardening, which is expected to play an appreciable role on the springback of the piece when the stamping tools are removed [1].

The constant work contours (CWCs) are defined in stress space by joining the points obtained under different quasi-linear strain-paths or stress states at a given value of expended plastic work. With the CWCs, emphasis is given to initial anisotropy and to possible differential hardening effects that manifest by differences in strain-hardening along different strain-paths, leading to an evolution of the shape of the CWCs with the level of plastic work. Experimental evidence [2] tends to indicate that the directions of plastic strain increments are

normal to the CWCs, which explains that they are commonly modeled by a yield function and its associated flow rule. Among many anisotropic yield functions proposed during the last decades, Hill's quadratic function [3] is the best known and remains the most widely used in industrial context.

The present paper focuses on the experimental methods that can be used to identify anisotropic yield surfaces and/or CWCs, which play a prominent role in the predictions of strain distributions and defects in the formed part. Two main methods are examined : first, direct methods for identifying the CWCs, in which a variety of tests are performed to cover a wide range of linear or quasi-linear strain-paths (see also the excellent review on sheet metals experimental characterization by Kuwabara [4]) ; second, inverse methods using experiments on complex-shaped specimens, where the parameters of a material model are determined by minimizing the discrepancies between numerically-predicted results and experimental ones.

2 DIRECT IDENTIFICATION METHODS

Direct identification methods of the three-dimensional plastic behavior of metals were developed concurrently with modern plasticity theories. A pioneering example is given by the work of Lode [5], who tested thin tubes under combined axial tension and internal pressure in order to examine the influence of the intermediate principal stress on yielding. A number of tests covering a wide range of biaxial stress states have also been proposed for a long time for sheets in order to define an appropriate anisotropic yield function fitting experimental data. These classical tests are critically reviewed in this section, together with more recent experiments conducted on biaxially stretched specimens.

2.1 Uniaxial tension tests

The uniaxial tension test is accepted as an unquestionable experiment for characterizing strain-hardening and plastic anisotropy. Its main limitation comes from the occurrence of necking, which restricts its straightforward analysis to strain levels corresponding to the point of maximum load. An example of uniaxial stress-strain curves taken from [6] is given on Fig. 1a for annealed 1050A aluminum specimens cut along the rolling direction (RD), the diagonal direction (DD) and the transverse direction (TD). The total logarithmic surface strains ε_1 and ε_2 along the tensile and the width directions, respectively, were determined during the tests as the average values obtained over a central zone of the specimens by using an image correlation method. The Lankford coefficient R measuring the ratio between plastic strains in the width direction (ε_2^p) and in the thickness direction (ε_3^p) was then calculated by taking into account the contribution of elastic strains and the assumption of plastic incompressibility. The evolutions of R as a function of plastic strain ε_1^p along the tensile direction are shown on Fig. 1b. It can be observed that the stress-strain curve along TD exhibits a slightly lower hardening rate, as compared to RD and DD, Fig. 1a. Besides, the Lankford coefficient slightly evolves during the tests, Fig. 1b. These observations indicate that the assumption of isotropic hardening is not rigorously satisfied.

The angular variations of the Lankford coefficient (measured at $\varepsilon_1^p = 0.1$) and of the flow stress at different values of plastic work are shown on Figs 1c and 1d, respectively. The

relation between strain anisotropy, Fig. 1c, and stress anisotropy, Fig. 1d, cannot be accounted for with Hill's quadratic criterion [3], which only involves 3 parameters for describing the adimensional plane-stress yield surface. The FMM model proposed by Ferron et al. [7] is used in Fig. 1d to fit the variations of both $R(\alpha)$ and $\sigma(\alpha)$.

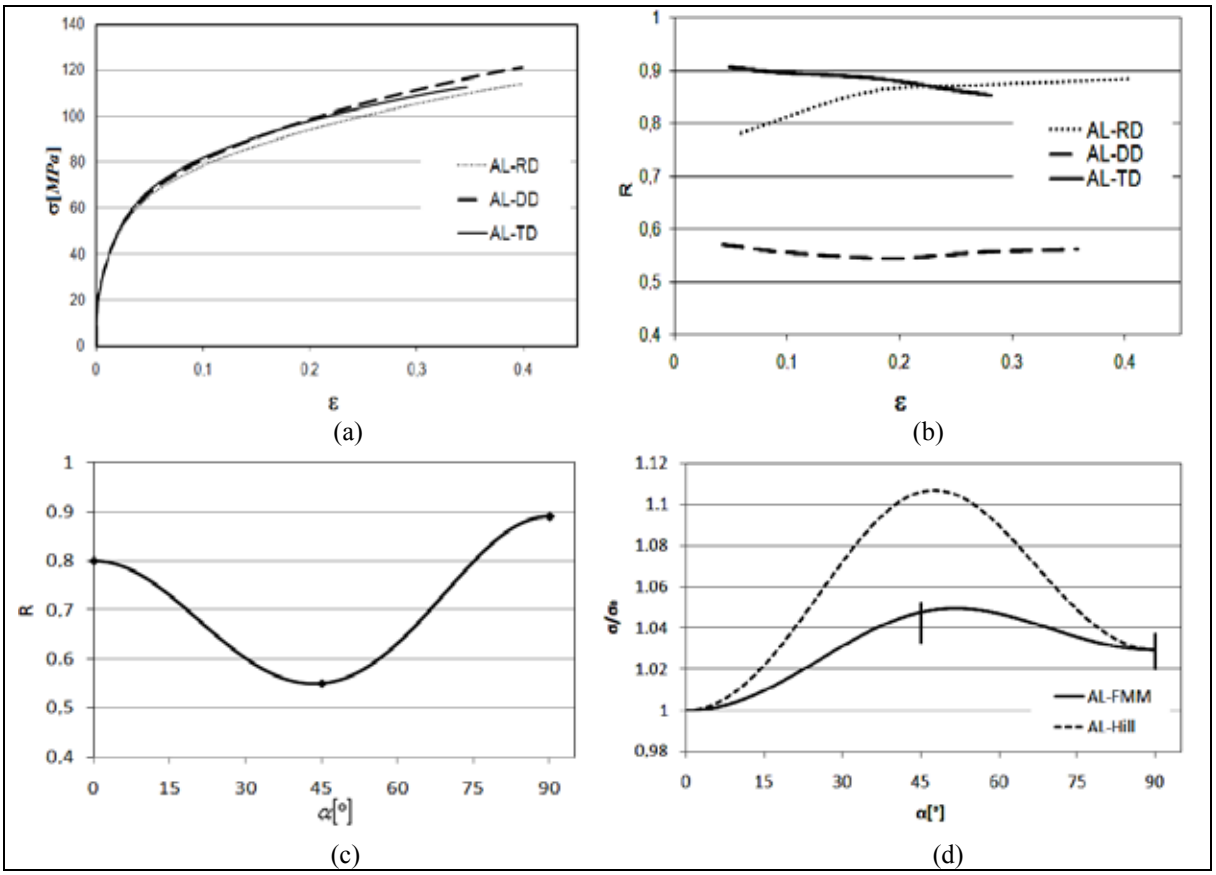

Figure 1: Uniaxial stress-strain curves (a), evolution of the Lankford coefficient (b), and angular variations of the Lankford coefficient (c) and of normalized flow stress (d) for annealed 1050A aluminum (after [6]).

More complex angular evolutions of the Lankford coefficient and of the flow stress can be obtained in dual phase steels [8] or in aluminum alloys [9]. An asymmetric yield behavior in tension and compression can also be observed in some advanced materials [9].

2.2 Shear tests

The simple shear test can be performed on a conventional testing machine by means of a device imposing a parallel displacement of two lateral grips, which leads to a shear strain γ as shown on Fig. 2a (from [10]). Compared with the uniaxial tension test, much larger homogeneous strains can be obtained with this test. Also, the stress can easily be reversed by inverting the relative displacement of the grips. Further flexibility for analyzing strain-induced anisotropy is obtained by cutting samples in prestrained sheets [10]. Simple shear results are illustrated on Fig. 2b for a low-carbon steel with 20% tension prestrain along RD.

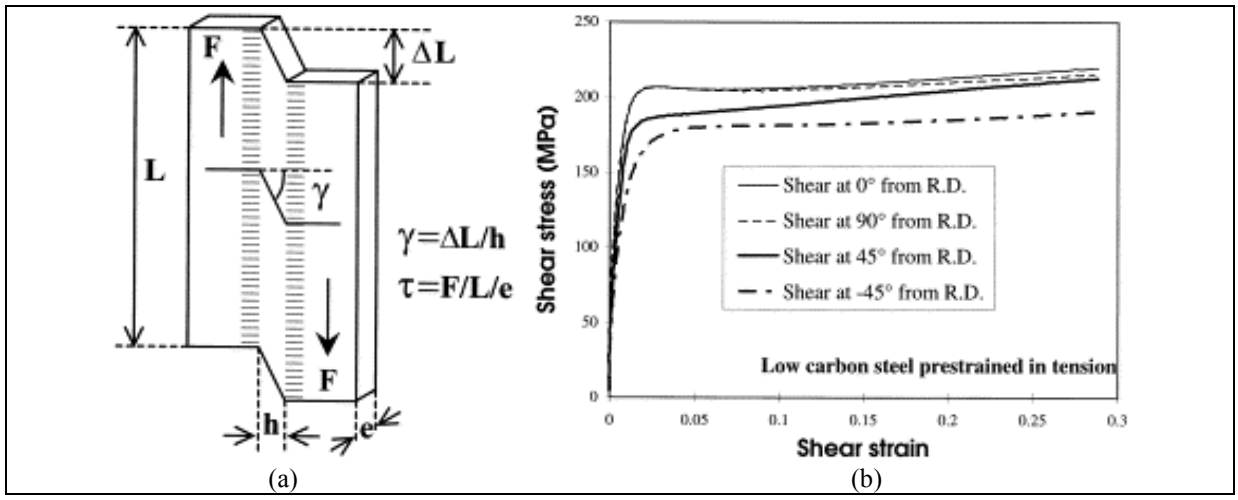

Figure 2: Geometry of a simple shear sample (a) and experimental shear stress–shear strain curves for a low-carbon steel after 20% prestrain in tension along RD (b) (from [10]).

2.3 Plane-strain tension tests

The tension test on wide specimens (Fig. 3a) can be used to obtain strain states close to plane-strain tension in the middle section of minimal cross-sectional area [11]. With the assumption of plane-strain tension, the plane-strain stress-strain curve can be directly estimated by recording the load and the (average) axial strain in the middle section. However, an extensive study by Dournaux et al. [12] clearly shows that uniform stress- and strain-states are not obtained in the middle section. Strain field analysis by means of optical full-field measurement techniques further shows that the degree of strain field homogeneity is strongly sensitive to specimen geometry. An optimized geometry can be searched by FE analysis, but the results depend on the yield function [12]. Finally, this test could alternatively be used to analyze the ability of selected constitutive models to reproduce the inhomogeneous strain fields.

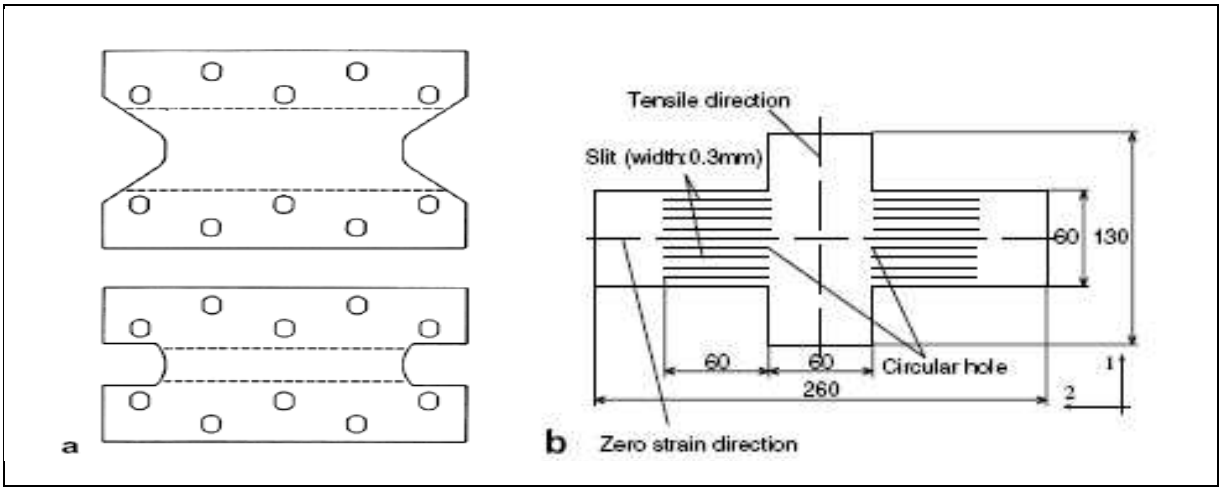

Figure 3: Plane-strain tension wide specimens proposed by Wagoner [11] (a);
plane-strain tension cruciform specimen proposed by Kuwabara and Ikeda [13] (b).

Cruciform specimens (Fig. 3b) also have been designed for plane-strain stretching, with slits machined along the direction normal to the loading direction, while the elongation along this normal direction is maintained equal to zero during the test [13].

2.4 Bulge test

Following the earlier work of Mellor [14], the plastic bulging of a blank clamped along a circular contour and submitted to the action of a lateral fluid pressure is widely used in industrial and academic laboratories. Large plastic strains are obtained with this test at the apex of the dome. The biaxial flow stress σ_b at the apex is estimated by measuring fluid pressure p and calculating the thickness and curvatures at the pole, via appropriate measurements and assumptions. The surface strains ε_1 and ε_2 and curvatures $(1/R_1)$ and $(1/R_2)$ along RD and TD, respectively, are determined as average values measured over a certain area around the pole by means of either extensometers and spherometers, or optical systems allowing a continuous recording of the coordinates of a grid applied on the sheet. The through-thickness strain ε_3 is estimated with the assumption of incompressibility :

$$\varepsilon_3 = -(\varepsilon_1 + \varepsilon_2) \tag{1}$$

and the thickness t is determined as :

$$t = t_0 \exp(\varepsilon_3) \tag{2}$$

where t_0 is the initial thickness.

The biaxial stress at the pole is determined using the membrane equilibrium equation :

$$\frac{\sigma_1}{R_1} + \frac{\sigma_2}{R_2} = \frac{p}{t} \tag{3}$$

where σ_1 and σ_2 are the membrane stresses.

The local shape of the deformed sheet around the pole is often approximated by a sphere. Then, under the assumptions $R_1 \approx R_2 \equiv R$ and $\sigma_1 \approx \sigma_2 \equiv \sigma_b$, equation (3) reduces to :

$$\sigma_b = \frac{pR}{2t} \tag{4}$$

Apart from experimental accuracy, several elements can affect the determination of the biaxial stress-strain law. First, the strain and the curvature depend on the position along the profile. Thus, the determination of surface strains and curvatures at the pole may depend on the size of the zone used for their determination. Second, the determination of the thickness using the strains measured on the upper face of the sheet ignores the strain gradients through the thickness, which arise from the combination of stretching and bending for thick sheets. Third, the membrane equilibrium equations (3) and (4) represent an approximation for thick sheets.

In order to evaluate the accuracy of the bulge test analysis, Lemoine et al. [15] performed virtual experiments in which the results obtained by FE calculations are used as input data for determining the biaxial stress-strain law in agreement with the experimental procedure. In this way, the experimental procedure can be evaluated by comparing the "experimental" stress-strain curve with the "reference" one introduced in the simulations. The $\sigma_1(|\varepsilon_3|)$ curves predicted for an isotropic (von Mises) material with a die diameter of 108 mm and for different sheet thicknesses are shown on Fig. 4a. A progressive overestimate of the stress-strain curve is observed with the experimental determination. This effect is more significant for materials with a lower hardening rate, and it is clearly much more important for thick sheets. The strain gradients through the thickness partly explain this effect, as a result of a progressive underestimate of the thickness when it is computed with the value of the upper surface strain ε_1 [15]. For thick sheets, it is also observed that the calculated stress is far too low in the early stages of bulging (Fig. 4a). This effect can be explained by the initial predominance of bending. This may be observed on Fig. 4b where the evolution of stress σ_1 at the apex is plotted as a function of dome height *H* for different nodes through the thickness of the sheet.

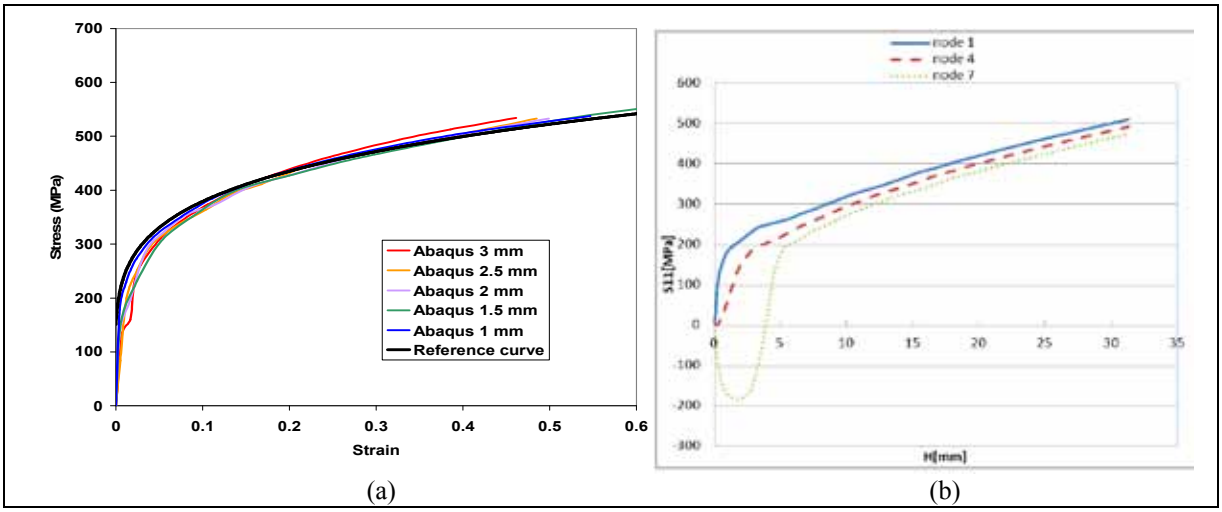

(a) (b)

Figure 4: Comparison between the "reference" curve and "experimental" curves (Abaqus) for different thicknesses (a); evolution of apex stress σ_1 as a function of dome height *H* for the upper node 1, mid node 4 and lower node 7 through the thickness (b) (from [15]).

For in-plane anisotropic materials, the approximation $\sigma_1 = \sigma_2$ in the equilibrium equation (4) is an additional source of error, because the strain and stress states at the apex neither exactly correspond to equibiaxial states [15].

2.5 Compression tests

Biaxial compression tests can be performed on adhesively bonded blocks of sheet specimens [16]. Generally, these tests are analyzed by assuming pressure-insensitive plastic yielding, which allows the direct prediction of in-plane loading behavior. Some difficulties

possibly arise from friction, from lack of parallelism between the specimen and the tools and from elasticity effects [17].

2.6 Biaxial tension tests

Reviews of cruciform specimens designed for determining yield stress or stress-strain curves in biaxial tension can be found in [4,18]. Some examples of cruciform specimens are shown on Fig. 5. With these specimens, a direct identification of the stress-strain law in biaxial tension is performed by measuring the deformation in the central gauge part and by determining the stress from equilibrium considerations. The main difficulty with this kind of specimens consists of obtaining significant levels of biaxial stretching in the central part. This difficulty can be overcome by machining slits in the specimen arms and creating a thinner central part [20,21]. Kuwabara et al. [2] avoided this thinning by machining very narrow slits in the arms, so that the cross-sectional area of arms is almost the same as that of the central gauge part. However, the amount of stretching in the central part is limited in this case to a few percents of elongation.

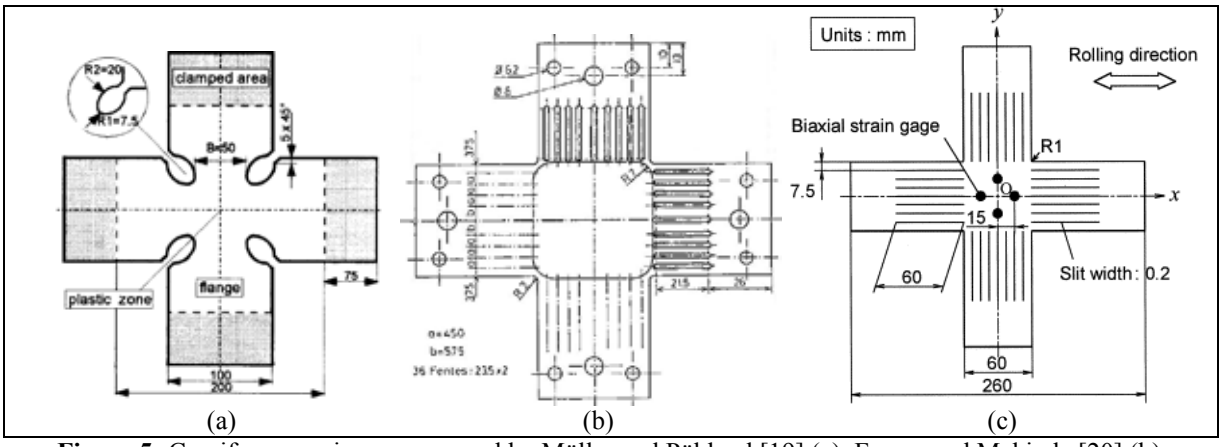

(a) (b) (c)

Figure 5: Cruciform specimens proposed by Müller and Pöhland [19] (a), Ferron and Makinde [20] (b) and Kuwabara et al. [2] (c).

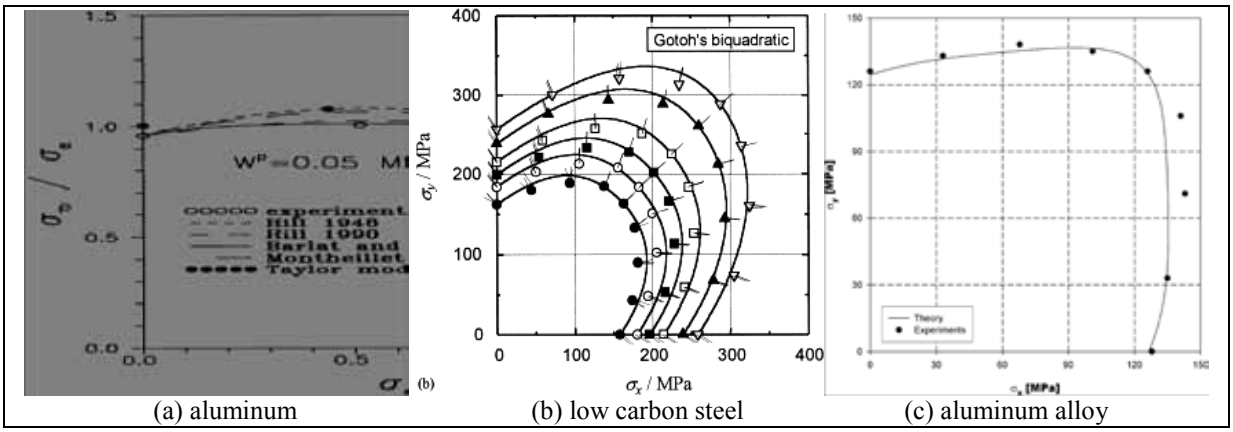

(a) aluminum (b) low carbon steel (c) aluminum alloy

Figure 6: Constant works contours determined with cruciform specimens by Green et al. [22] (a), Kuwabara et al. [2] (b) and Banabic et al. [23] (c).

Examples of CWCs determined in the biaxial stretching range are shown on Fig. 6. The biaxial devices used for these experiments consist of two sets of opposite actuators, which are servo-controlled at either a given strain ratio [22] or a given load ratio [2,23] to obtain one point of the CWC. Referring to the denominations used in Fig. 5, specimens are of either type (b) [22] or type (c) [2,23].

3 INVERSE IDENTIFICATION METHODS

Inverse identification methods are carried out by using an optimization procedure in which the parameters of the constitutive law introduced in FE simulations are adjusted in order to minimize the discrepancies between numerically predicted results and experimental ones. Theoretical formulations of the identification problem can be found in [24,25]. For plastically deformed anisotropic sheet metals, the global results related to the load-displacement response were first analyzed. Owing to the advances in optical full-field measurement techniques, the analysis of heterogeneous strain fields obtained on specifically-designed specimens is now increasingly used for the identification of material parameters.

3.1 Global results analysis

Load-displacement results have been analyzed in a variety of situations by Ghouati and Gelin [25] to identify strain-hardening parameters and Hill's quadratic yield function parameters. Experiments used for identification include uniaxial tension tests, bulge tests and deep-drawing tests. Another example of global results analysis is given in [26], where plane-strain tension tests are analyzed by recording the load as a function of the thickness in the centre of the specimen. Plastic yielding is modeled using Hill's quadratic model with the assumptions of either associated or non-associated flow rule, and Barlat's yield function (Yld91) [27]. Improved results could be obtained with this latter yield function.

3.2 Strain fields analysis

More informative and discriminant results are expected from full-field displacement and strain measurements. One of the first studies using full-field displacement measurements on plastically-stretched sheet metals was performed by Meuwissen et al. [28]. These authors designed non-standard tensile specimens with dissymmetric notches (Fig. 7a). The displacement fields were measured optically with retro-reflective markers on the specimen surface. Belhabib et al. [29] also used notched specimens (Fig. 7b). These authors performed full-field optical strain measurements and FE analysis to determine the strain-hardening parameters and Hill's quadratic yield function parameters. Kajberg and Lindkvist [30] performed a numerical optimization of strain measurements on notched specimens with the aim of determining the stress-strain law at large strains.

A much wider range of stress states can be covered using biaxially-stretched cruciform specimens. For a pertinent identification based on strain fields analysis, the design of cruciform specimens should be guided by the following prescriptions [31]:

- obtain a wide range of stress-states over the surface of the specimen,
- obtain a satisfactory compromise between a significant strain level in all the regions of the specimen and a high sensitivity of strain fields to plastic anisotropy.

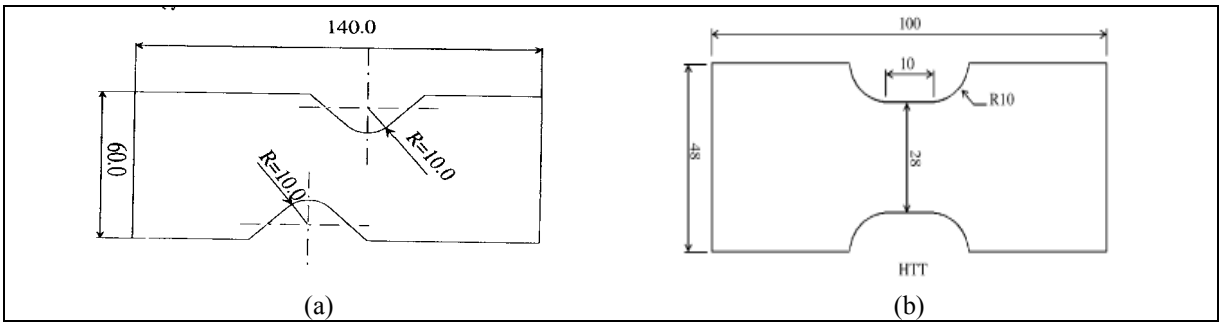

Figure 7: Non-standard tensile specimens designed by Meuwissen et al. [28] (a) and Belhabib et al. [29] (b).

Two types of cruciform specimens designed according to the above objectives [31,32] are presented on Fig. 8. Both types exhibit the same external shape. The geometry of the first type is simply defined by a hole machined in its centre (Fig. 8a). The stress-state is close to uniaxial tension in the major part of specimen arms (UT region), and close to plane-strain tension along the lines oriented at 45° from the specimen axes (PST region). The second type of specimens (Fig. 8b) is designed to enforce different stress states along the symmetry axes:

- equibiaxial tension (EBT) in the centre of the specimen, defined by the Lagrangian coordinate $X = 0$,
- plane-strain tension (PST) at the points at $X \approx \pm 10\,\text{mm}$, where a strain peak is observed between the ends of the slots oriented at 45° from the symmetry axes,
- uniaxial tension (UT) in the regions defined by $25\ \text{mm} < |X| < 40\ \text{mm}$, where a strain plateau is observed along the central ligaments of the arms.

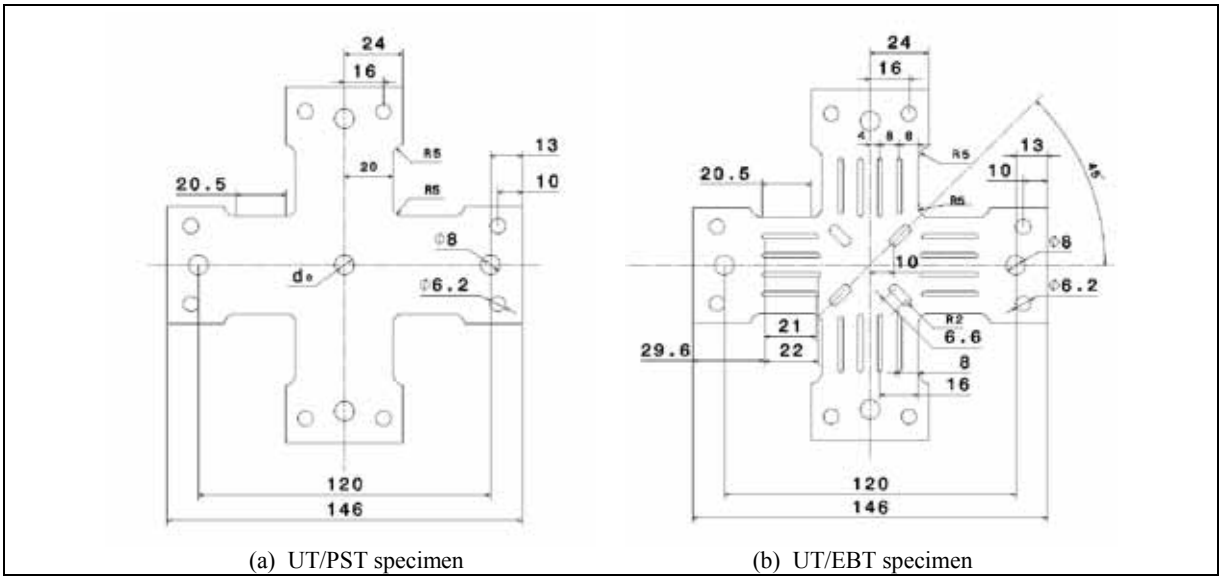

Figure 8: Cruciform specimens with stress states ranging from uniaxial tension to plane-strain tension (a) and from uniaxial tension to equibiaxial tension (b) [31,32].

The identification procedure [31,32] is performed with a 8-parameter yield function [7] by combining the results of uniaxial tension tests and biaxial tension tests on cruciform

specimens. Uniaxial tension tests along the directions at 0°, 45° and 90° from the rolling direction are carried out to determine the strain-hardening parameters and yield function parameters related to transverse strain- and stress-anisotropy. Strain distributions measured in biaxial tension tests by an image correlation method are used as input data in an optimization procedure allowing the determination of yield function parameters related the shape of the yield surface in biaxial tension. As an illustration, the plot of major principal strains measured for various materials along the symmetry axis corresponding to the rolling direction of UT/EBT specimens (Fig. 9a) displays the high sensitivity of strain fields to material anisotropy. The yield surfaces obtained by the identification procedure are shown on Fig. 9b.

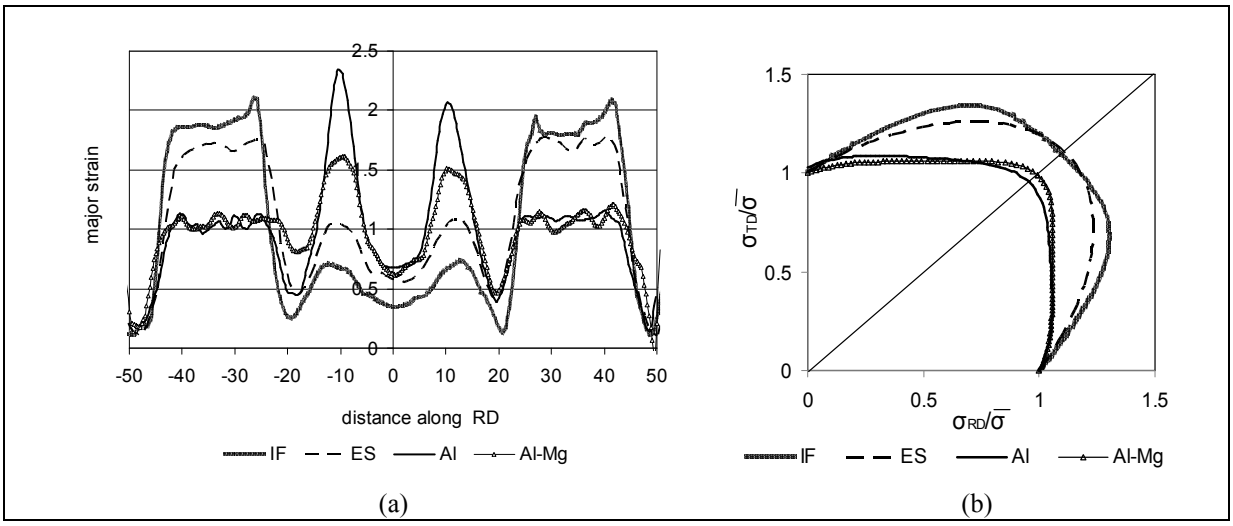

Figure 9: Normalized distributions of major principal strain measured along the rolling direction of UT/EBT specimens (a) and identified yield surfaces in the biaxial stretching range (b) (from [31]).

4 CONCLUSIONS

The aspects of sheet metals plastic anisotropy reviewed in this paper mainly deal with the experimental identification of yield surfaces, and more specifically of constant work contours. To improve numerical predictions of strain distributions and to assess the feasibility of a forming process, these experiments should bring accurate information about:

- the *orientation* dependence of yielding, both concerning transverse *strain*- and *stress*-anisotropy, which plays a prominent role in processes with draw-in, as is the case for the formation of ears in the cup drawing test,
- the *stress-ratio* dependence of yielding, particularly the shape of the yield surface in the biaxial stretching range, which controls the strain distributions obtained in stampings that present a wide range of stress states. The use of biaxially stretched specimens, designed either for a direct or an inverse identification, represents an efficient mean for this characterization.

The yield surfaces can be modeled by choosing one of the anisotropic yield functions developed during the last 30 years concurrently with ever more accurate characterizations of sheet yielding, see, e.g., the reviews of Banabic [33] and Barlat et al. [34].

REFERENCES

[1] B. Tang, X. Lu, Z. Wanga and Z. Zhao, "Springback investigation of anisotropic aluminum alloy sheet with a mixed hardening rule and Barlat yield criteria in sheet metal forming", *Materials and Design*, **31**: 2043-2050 (2010).

[2] T. Kuwabara, S. Ikeda and K. Kuroda, "Measurement and analysis of differential work hardening in cold-rolled steel sheet under biaxial tension", *J. Mater. Proc. Technol.*, **80-81**: 517-523 (1998).

[3] R. Hill, "A theory of the yielding and plastic flow of anisotropic metals", *Proc. Royal Soc. London*, **A193**: 281-297 (1948).

[4] T. Kuwabara, "Advances in experiments on metal sheets and tubes in support of constitutive modeling and forming simulations", *Int. J. Plast.*, **23**: 385-419, (2007).

[5] W. Lode, "Versuche über den Einfluss der mittleren Hauptspannung auf das Fliessen der Metalle Eisen, Kupfer und Nickel", *Z. Physik*: **36**, 913 (1926).

[6] M. Teaca, "Caractérisation expérimentale et modélisation de la déformation plastique des tôles métalliques", *PhD thesis*, Metz (2009).

[7] G. Ferron, R. Makkouk and J. Morreale, "A parametric description of orthotropic plasticity in metal sheets", *Int. J. Plast.*, **10**: 431-449 (1994).

[8] M. Rabahallah, T. Balan, S. Bouvier, B. Bacroix, F. Barlat, K. Chun and C. Teodosiu, "Parameter identification of advanced plastic strain rate potentials and impact on plastic anisotropy prediction", *Int. J. Plast.*, **25**: 491-512, (2009).

[9] B. Plunkett, O. Cazacu and F. Barlat, "Orthotropic yield criteria for description of the anisotropy in tension and compression of sheet metals", *Int. J. Plast.*, **24**: 847-866 (2008).

[10] E.F. Rauch, "Plastic anisotropy of sheet metals determined by simple shear tests", *Mat. Sci. Engng*, **A241**: 179-183 (1998).

[11] R.H. Wagoner, "Measurement and analysis of plane-strain work hardening", *Met. Trans.*, **11A**: 165-175 (1980).

[12] J.L. Dournaux, S. Bouvier, A. Aouafi and P. Vacher, "Full-field measurement technique and its application to the analysis of materials behavior under plane-strain mode", *Mat. Sci. Engng*, **A500**: 47-62 (2009).

[13] T. Kuwabara and S. Ikeda, "Measurement and analysis of work hardening of sheet steels subjected to plane strain tension", *Tetsu-to-Hagane*, **88 (6)**: 334-339 (2002).

[14] P.B. Mellor, "Stretch forming under fluid pressure", *J. Mech. Phys. Solids*, **5:** 41-56 (1956).

[15] X. Lemoine, A. Iancu and G. Ferron, "Flow curve determination at large plastic strain levels: limitations of the membrane theory in the analysis of the hydraulic bulge test", *Esaform 2011*, Belfast, 27-29 april 2011.

[16] Y. Tozawa, "Plastic deformation behavior under the compression of combined stress", in *Mechanics of Sheet Metal Forming*, eds D.P. Koistinen and N.M. Wang, pp. 81-110, Plenum Press, New York (1978).

[17] Y. Maeda, M. Yanagawa, F. Barlat, K. Chung, Y. Hayashida, S. Hattori, K. Matsui, J.C. Brem, D.J. Lege, S.J. Murtha and T. Ishikawa, "Experimental analysis of aluminum yield surface for binary Al-Mg alloy sheet samples", *Int. J. Plast.*: **14**, 301-318 (1998).

[18] A. Hannon and P. Tiernan, "A review of planar biaxial tensile test systems for sheet metal", *J. Mater. Proc. Technol.*, **198**: 1-13 (2008).
[19] W. Müller and K. J. Pöhlandt, "New experiments for determining yield loci of sheet metal", *J. Mater. Process. Technol.*, **60**: 643-648 (1996).
[20] G. Ferron and A. Makinde, "Design and development of a biaxial strength testing device", *J. Test. Evaluat.*, **16**: 253-256 (1988).
[21] J.P. Boehler, S. Demmerle and S. Koss, "A new direct biaxial testing machine for anisotropic materials", *Exp. Mech.*, **34**: 1-9 (1994).
[22] D.E. Green, K.W. Neale, S.R. MacEwen, A. Makinde and R. Perrin, "Experimental investigation of the biaxial behaviour of an aluminum sheet", *Int. J. Plast.*, **20**: 1677-1706 (2004).
[23] D. Banabic, T. Kuwabara, T. Balan, D.S. Comsa and D. Julean, "Non-quadratic yield criterion for orthotropic sheet metals under plane-stress conditions", *Int. J. Mech. Sci.*, **45**: 797-811 (2003).
[24] R. Mahnken and E. Stein, "A unified approach for parameter identification of inelastic material models in the frame of the finite element method", *Computer Methods Appl. Mech. and Engng*, **136**: 225-258 (1996).
[25] O. Ghouati and J.C. Gelin, "A finite element-based identification method for complex metallic material behaviour", *Comput. Mater. Sci.*, **21**: 57-68 (2001).
[26] A. Khalfallah, H. Bel Hadj Salah and A. Dogui, "Anisotropic parameter identification using inhomogeneous tensile test", *Eur. J. Mech. A/Solids*, **21**: 927-942 (2002).
[27] F. Barlat, D.J. Lege and J.C. Brem, "A six-component yield function for anisotropic materials", *Int. J. Plast.*, **7**: 693-712 (1991).
[28] M.H.H. Meuwissen, C.W.J. Oomens, F.P.T. Baaijens, R. Petterson and J.D. Janssen, "Determination of the elasto-plastic properties of aluminium using a mixed numerical-experimental method", *J. Mater. Process. Technol.*, **75**: 204-211 (1998).
[29] S. Belhabib, H. Haddadi, M. Gaspérini and P. Vacher, "Heterogeneous tensile test on elastoplastic metallic sheets: Comparison between FEM simulations and full-field strain measurements", *Int. J. Mech. Sci*., **50**: 14-21 (2008).
[30] J. Kajberg and G. Lindkvist, "Characterisation of materials subjected to large strains by inverse modeling based on in-plane displacement fields", *Int. J. Solids Struct.*, **41**: 3439-3459 (2004).
[31] M. Teaca, M. Martiny, I. Charpentier and G. Ferron, "Heterogeneous biaxial tensile tests for the characterization of sheet metals plastic anisotropy", *AIP Conference Proceedings* **1315:** 57-62 (2011).
[32] M. Teaca, I. Charpentier, M. Martiny and G. Ferron, "Identification of sheet metal plastic anisotropy using heterogeneous biaxial tensile tests", *Int. J. Mech. Sci*., **52**: 572-580 (2010).
[33] D. Banabic, "Formability of metallic materials", Springer, Heidelberg (2000).
[34] F. Barlat, J.W. Yoon and O. Cazacu, "On linear transformations of stress tensors for the description of plastic anisotropy", *Int. J. Plast.*, **23**: 876-896 (2007).